

Spontaneous and stimulated emission tuning characteristics of a Josephson junction in a microcavity

Andrea T. Joseph, Robin Whiting and Roger Andrews

Department of Physics, University of the West Indies, St. Augustine, Trinidad and Tobago

randrews@fans.uwi.tt

We have investigated theoretically the tuning characteristics of a Josephson junction within a microcavity for one-photon spontaneous emission and for one-photon and two-photon stimulated emission. For spontaneous emission, we have established the linear relationship between the magnetic induction and the voltage needed to tune the system to emit at resonant frequencies. For stimulated emission, we have found an oscillatory dependence of the emission rate on the initial Cooper pair phase difference and the phase of the applied field. Under specific conditions, we have also calculated the values of the applied radiation amplitude for the first few emission maxima of the system and for the first five junction-cavity resonances for each process. Since the emission of photons can be controlled, it may be possible to use such a system to produce photons on demand. Such sources will have applications in the fields of quantum cryptography, communications and computation.

OCIS codes: (999.9999) Josephson junction; microcavity; spontaneous emission; stimulated emission

1. Introduction

Since the earlier half of the twentieth century, confined atoms have been studied both theoretically¹ and experimentally². The interaction of these atoms or molecules with confined electromagnetic fields has always garnered a great deal of attention.^{3,4} The field of Cavity

Quantum Electrodynamics (QED) deals with the study of such interactions in cavities.^{5,6} Moreover, very often, these investigations involve the use of two-level atoms.^{7,8} In 1970 and in 1976 respectively, Tilley,⁹ and Rogovin and Scully¹⁰ had presented theoretical studies illustrating the analogy between a Josephson junction and a two-level atom. The first experimental confirmation of their predictions came in 1999.¹¹ In this study, measurements were made of 150 GHz electromagnetic radiation emitted by three two-dimensional Josephson junction arrays. Each array was comprised of underdamped Nb / Al / AlO_x / Nb Josephson tunnel junctions and each junction was coupled to a high-Q cell resonance. The arrays emitted coherently above a threshold that increased as the array size increased and the detected ac power exhibited an N^2 dependence, where N represented the number of active junctions in the array. They also observed synchronization between incoming radiation and radiation emitted by the junctions. Even before this publication though, there had already been research carried out on the interaction of Josephson junctions with cavities.¹² Since 1999 other articles detailing analyses of Josephson junction-cavity systems have also been published.^{13,14}

In this paper, Rogovin and Scully's model of the Josephson junction as a two-level atom is used to investigate specifically the spontaneous and stimulated emission of radiation from a Josephson junction within a microcavity. For spontaneous emission, the Hamiltonian employed uses the classical form of the pair current density for the junction in the presence of an applied static magnetic field and a DC voltage. For stimulated emission, with the junction placed in an external electromagnetic field and biased at a DC voltage, the form of the photon-assisted pair current density for the junction is used. The Josephson junction is assumed to be much smaller than the cavity length. The one-photon process is investigated for spontaneous emission and the one-photon and two-photon processes for stimulated emission. Relevant equations are presented to calculate the parameters necessary to achieve resonance for spontaneous emission and

magnitudes of parameters needed to produce maximum count rates for stimulated emission are calculated.

2. Interaction Hamiltonian and field quantisation for a Josephson junction in a microcavity

The Josephson junction under consideration, is comprised of an insulating layer of thickness l sandwiched between two superconducting layers and has been given a length L .

The resultant interaction Hamiltonian¹⁵ describing the coupling of the electron pairs to the electromagnetic field is given as

$$\hat{H}_i = \frac{1}{c_o} \int d^3r \mathbf{j}(\mathbf{r}) \cdot \hat{\mathbf{A}}(\mathbf{r}, t), \quad (1)$$

where c_o is the speed of the electromagnetic radiation in the insulating layer, $\mathbf{j}(\mathbf{r})$, the pair current density, and $\hat{\mathbf{A}}(\mathbf{r}, t)$, the electromagnetic vector potential.

The Josephson junction is placed in the microcavity such that it is centred at the origin (Fig. 1). In a cavity, the positive frequency part of the quantised vector potential is defined as¹⁶

$$\hat{\mathbf{A}}^+(\mathbf{r}, t) = \int d^3k \sum_j \left(\frac{\hbar}{16\pi^3 c_o k \epsilon'} \right)^{1/2} \boldsymbol{\varepsilon}(\mathbf{k}, j) [U_{\mathbf{k}j}(\mathbf{r}) \hat{a}_{\mathbf{k}j} + U'_{\mathbf{k}j}(\mathbf{r}) \hat{a}'_{\mathbf{k}j}] \exp(-i c_o k t). \quad (2)$$

$\boldsymbol{\varepsilon}(\mathbf{k}, j)$ represents the unit vector for the transverse polarization directions where $j = 1, 2$ and ϵ' is the permittivity of the medium of the cavity and insulating layer. The wave vectors can be either \mathbf{k}_+ or \mathbf{k}_- , where \mathbf{k}_+ is used for modes propagating to the right and \mathbf{k}_- , for those to the left. They are defined as¹⁶

$$\mathbf{k}_{\pm} = k(\sin \theta \cos \phi, \sin \theta \sin \phi, \pm \cos \theta), \quad (3)$$

where θ ($0 < \theta < \pi/2$) and ϕ ($0 < \phi < 2\pi$) are the spherical angles. $U_{\mathbf{k}j}(\mathbf{r})$ and $U'_{\mathbf{k}j}(\mathbf{r})$ are the spatial mode functions of the cavity. $\hat{a}_{\mathbf{k}j}^+$ and $\hat{a}_{\mathbf{k}j}$ [$\hat{a}'_{\mathbf{k}j}^+$ and $\hat{a}'_{\mathbf{k}j}$] are the creation and destruction operators, respectively, for the mode with spatial function $U_{\mathbf{k}j}(\mathbf{r})$ [$U'_{\mathbf{k}j}(\mathbf{r})$].

The geometrical details of the Fabry-Perot microcavity used in this investigation are given in Fig. 2. The mirrors of the cavity, assumed to be ideal, with zero thickness and absorption, extend infinitely in the $x-y$ plane. The z -axis is perpendicular to the plane of the mirrors and the origins of the x , y and z axes are at the centre of the cavity.

The Josephson junction wave function, $|\psi_J\rangle$, is the direct product of the BCS wave functions for the upper and lower superconducting layers.¹⁰ For the lower layer,

$$|\psi_n\rangle = |\mathbf{q}\uparrow, -\mathbf{q}\downarrow\rangle = \prod_{\mathbf{q}} (u_{\mathbf{q}} + v_{\mathbf{q}} C_{\mathbf{q}\uparrow}^+ C_{-\mathbf{q}\downarrow}^+) |0\rangle, \quad (4)$$

and for the upper superconducting layer,

$$|\psi_m\rangle = |\mathbf{s}\uparrow, -\mathbf{s}\downarrow\rangle = \prod_{\mathbf{s}} (u_{\mathbf{s}} + v_{\mathbf{s}} C_{\mathbf{s}\uparrow}^+ C_{-\mathbf{s}\downarrow}^+) |0\rangle, \quad (5)$$

where $(\mathbf{s}\uparrow, -\mathbf{s}\downarrow)$ [$(\mathbf{q}\uparrow, -\mathbf{q}\downarrow)$] represents the pair state of the electron pairs in the upper [lower] superconducting layer, and $C_{\mathbf{s}\uparrow}^+$ and $C_{-\mathbf{s}\downarrow}^+$ [$C_{\mathbf{q}\uparrow}^+$ and $C_{-\mathbf{q}\downarrow}^+$] are the creation operators for the electrons in the Bloch states $|\mathbf{s}\uparrow\rangle$ and $|\mathbf{s}\downarrow\rangle$ [$|\mathbf{q}\uparrow\rangle$ and $|\mathbf{q}\downarrow\rangle$] respectively. $u_{\mathbf{s}}$ [$v_{\mathbf{s}}$] is the probability amplitude that the pair state $(\mathbf{s}\uparrow, -\mathbf{s}\downarrow)$ is empty [filled]. $|\psi_J\rangle$ is given as $|\psi_n\rangle \times |\psi_m\rangle$, and the part of $|\psi_J\rangle$ that describes pair tunneling would include terms containing $C_{\mathbf{s}\uparrow}^+ C_{-\mathbf{s}\downarrow}^+$ and $C_{\mathbf{q}\uparrow}^+ C_{-\mathbf{q}\downarrow}^+$. For electrons with energy $\bar{\epsilon}_{\mathbf{q}}$, where $\bar{\epsilon}_{\mathbf{q}}$ is the electron energy relative to

the Fermi energy, such that $-\hbar\omega_D < \bar{\epsilon}_q < \hbar\omega_D$, $u_q = v_q = \frac{1}{\sqrt{2}}$, where ω_D is the Debye frequency of the metal. Additionally, the dynamics of the pair tunneling under investigation are such that electrons are transferred across the junction with no change in their wave vectors.

$|\psi_J\rangle$, can therefore be written as¹⁰

$$|\psi_J\rangle = \prod_s \frac{1}{2} [C_{s,\uparrow,m}^+ C_{-s,\downarrow,m}^+ + C_{s,\uparrow,n}^+ C_{-s,\downarrow,n}^+] |0\rangle. \quad (6)$$

3. Spontaneous emission

The initial state of the junction is given in Eq. (6) and no photons are present in the cavity. The initial state of the system, $|I_{sp}\rangle$, can therefore be written as

$$|I_{sp}\rangle = |\psi_{J_i}, 0\rangle, \quad (7)$$

where $|\psi_{J_i}\rangle$ represents the initial state of the Josephson junction. The final state, $|F_{sp}\rangle$, has the form

$$|F_{sp}\rangle = |\psi_{J_f}, 1\rangle, \quad (8)$$

where $|1\rangle$ indicates the presence of a photon in the final state and $|\psi_{J_f}\rangle$ represents the final state of the junction.

The probability amplitude that the system, at time t is in the state $|F\rangle$ is to first order in perturbation theory

$$-\frac{i}{\hbar} \int_{t_0}^t \langle F | \hat{H}_i | I \rangle dt' \quad (9)$$

where $|I\rangle$ and $|F\rangle$ are the initial and final states respectively.

Substituting Eq. (1) into Eq. (9), and using the expressions for the initial $|I_{sp}\rangle$ and final $|F_{sp}\rangle$ states for spontaneous emission, we obtain

$$-\frac{i}{\hbar c_o} \int_{t_o}^t \int d^3r [\langle \psi_{J_F} | \mathbf{j}(\mathbf{r}) | \psi_{J_I} \rangle \times \langle 1 | \hat{\mathbf{A}}(\mathbf{r}, t') | 0 \rangle] dt', \quad (10)$$

To generate electromagnetic radiation from the junction through the process of spontaneous emission, a DC voltage, V_o , is established across the insulating layer and a small static magnetic field¹⁷ is applied in the y -direction ($\mathbf{H}_o = 0, H_o, 0$). The presence of the voltage causes the supercurrent to oscillate at a frequency of $2eV_o/\hbar$ ¹⁸ and electromagnetic waves are radiated from the junction. For a magnetic field directed along the y -direction, the solution of the vector potential in the oxide and superconducting layers are such that the dominant component lies in the direction of current flow. This conclusion results from the analysis carried out by Swihart,¹⁹ and Eck, Scalapino and Taylor.²⁰ Due to the presence of the voltage and the magnetic field, the current component, $\langle \psi_{J_F} | \mathbf{j}(\mathbf{r}) | \psi_{J_I} \rangle$, of Eq. (10) can be written as¹⁰

$$j_1 \sin(\omega_o t' - k_o z). \quad (11)$$

j_1 is the pair current density amplitude and the Josephson frequency

$$\omega_o = 2eV_o/\hbar. \quad (12)$$

k_o is defined by the equation¹⁰

$$k_o = \frac{2e}{\hbar c_o} (2\lambda_L + l) H_o, \quad (13)$$

and represents the effect of the externally applied magnetic field on the tunnelling of the Cooper pairs. λ_L is the London penetration depth of the superconducting material and c_o is given by

$$c_o = \left[\frac{l}{\varepsilon(2\lambda_L + l)} \right]^{1/2} c. \quad (14)$$

The field component of Eq. (10) is given as

$$\left(\frac{\hbar}{16\pi^3 c_o \varepsilon'} \right)^{1/2} \langle 1 \left| \int d^3k \sum_j k^{-\frac{1}{2}} \varepsilon(\mathbf{k}, j) [U_{\mathbf{k}j}^*(z) \hat{a}_{\mathbf{k}j}^+ + U_{\mathbf{k}j}'^*(z) \hat{a}_{\mathbf{k}j}'^+] \exp(ic_o kt') \right| 0 \rangle, \quad (15)$$

where only the negative frequency part of the electromagnetic vector potential makes a non-zero contribution. The forms of the mode functions, $U_{\mathbf{k}j}(z)$ and $U_{\mathbf{k}j}'(z)$, in the region $-d/2 < z < d/2$ are as given below:¹⁶

$$U_{\mathbf{k}_+j}(z) = \frac{t_{1j} \exp(ikz \cos \theta)}{D_j}, \quad (16)$$

$$U_{\mathbf{k}_-j}(z) = \frac{t_{1j} r_{2j} \exp(ik(d-z) \cos \theta)}{D_j}, \quad (17)$$

$$U_{\mathbf{k}_+j}'(z) = \frac{t_{2j} r_{1j} \exp(ik(d+z) \cos \theta)}{D_j} \quad (18)$$

and

$$U_{\mathbf{k}_-j}'(z) = \frac{t_{2j} \exp(-ikz \cos \theta)}{D_j}, \quad (19)$$

where r_{1j} and t_{1j} [r_{2j} and t_{2j}] are the complex reflection and transmission coefficients for mirror 1 [2] respectively and

$$D_j \equiv 1 - r_{1j} r_{2j} \exp 2ikd \cos \theta. \quad (20)$$

The amplitude is calculated along the z-axis, i.e. $\theta \cong 0^\circ$. Another condition imposed is that mirror 1 is perfectly reflecting and mirror 2 highly reflecting, such that

$$r_{1j} = -1, \quad r_{2j} \rightarrow -1, \quad t_{1j} = 0, \quad t_{2j} \rightarrow 0. \quad (21)$$

Apart from constant factors, Eq. (15) is calculated to be

$$\int d^3k \left(k^{-\frac{1}{2}} \frac{\exp(ikz) - \exp(-ik(z+d))}{1 + r_{21}^* \exp(-2ikd)} \exp(ic_0 kt') \right). \quad (22)$$

Eq. (11) and Eq. (22) are then substituted into Eq. (10) and after carrying out the spatial and time integrations, the steady-state amplitude works out to be proportional to

$$\frac{\omega_n^{3/2} \sin \left[\left(k_o - \frac{\omega_n}{c_o} \right) \frac{L}{2} \right]}{\left(1 + r_{21}^* \exp \left(-\frac{2i\omega_n d}{c_o} \right) \right) \left(\left(k_o - \frac{\omega_n}{c_o} \right) \frac{L}{2} \right)} \exp \left(-\frac{i\omega_n d}{c_o} \right). \quad (23)$$

To calculate resonant frequencies, ω_n , that can be generated by the Josephson junction, the relation²¹

$$\omega_n = \frac{n\pi c_o}{L} \quad (24)$$

is used. By ensuring that the width, d , of the microcavity is an integral multiple of the length, L , of the Josephson junction, the resonant frequencies of the junction are resonant frequencies of the microcavity. From Eq. (23), there is resonance in the emission for

$$k_o \cong \frac{\omega_n}{c_o}. \quad (25)$$

This gives B_n as

$$B_n = \frac{\hbar \omega_n \mu_o}{2e(2\lambda_L + l)}, \quad (26)$$

where μ_o is the permeability of free space. For each value of ω_n calculated, the corresponding voltage, V_n , is obtained from

$$V_n = \frac{\hbar \omega_n}{2e}. \quad (27)$$

4. Stimulated emission

4.1 The one-photon process

To examine stimulated emission from the Josephson junction, a DC voltage, V_o , is maintained across the junction which is located in the microcavity in which there already exists an applied electromagnetic field. There is no static magnetic field present ($\mathbf{H}_o = 0$) and $j(\mathbf{r})$ is now of the form¹⁰

$$j = J_1 \sin \left[\omega_o t + \frac{2e}{\hbar\omega} V_1 \sin(\omega t + \theta') + \phi_o \right], \quad (28)$$

which, expressed in terms of Bessel functions, is re-written as

$$j = J_1 \sum_{s=-\infty}^{\infty} J_s \left(\frac{2eV_1}{\hbar\omega} \right) \sin[(\omega_o + s\omega)t + \phi_o + s\theta']. \quad (29)$$

J_1 represents the current density amplitude of the Cooper pairs and ω_o , the Josephson frequency. V_1 is the magnitude of the voltage induced by the applied field, ω , the frequency of the external radiation, θ' , the phase of the applied radiation and ϕ_o , the initial Cooper pair phase difference. $J_s(2eV_1/\hbar\omega)$ represents the ordinary Bessel function of order s and argument $2eV_1/\hbar\omega$.

To calculate the amplitude for stimulated emission, the Josephson junction-microcavity system is given an initial state such that one photon is present in the cavity and two photons are present in the final state. This is denoted respectively as

$$\begin{aligned} |I_{st}\rangle &= |\psi_{J_I}, 1\rangle, \\ |F_{st}\rangle &= |\psi_{J_F}, 2\rangle. \end{aligned} \quad (30)$$

$|I_{st}\rangle$ and $|F_{st}\rangle$ represent the initial and final states for stimulated emission.

The amplitude for stimulated emission is

$$-\frac{i}{\hbar c_o} \int_{t_o}^{t'} \int d^3 r [\langle \psi_{J_F} | j | \psi_{J_I} \rangle \times \langle 2 | \hat{A}_x(z, t') | 1 \rangle] dt', \quad (31)$$

After carrying out the various integrations, Eq. (31) works out to be proportional to

$$\frac{\omega_n^{1/2} \sin\left(\frac{\omega_n L}{2c_o}\right) \left(1 - \exp\left(-i \frac{\omega_n d}{c_o}\right)\right) \exp(-i\theta')}{\left(1 + r_{21}^* \exp\left(-i \frac{2\omega_n d}{c_o}\right)\right)} \left(J_{-2}\left(\frac{2eV_1}{\hbar\omega_n}\right) \exp(i\Delta\phi) - J_0\left(\frac{2eV_1}{\hbar\omega_n}\right) \exp(-i\Delta\phi) \right) \quad (32)$$

where ω_n represents resonant frequencies of the junction-cavity system. Here, again, ω_n is given by Eq. (24) and we are considering a situation where the resonant frequencies of the bare junction coincide with the resonant frequencies of the microcavity. $\Delta\phi$ is given as

$$\Delta\phi = \phi_o - \theta'. \quad (33)$$

To obtain Eq. (32), the applied microwave frequency is taken to be equal to one of the resonant frequencies of the system since we are considering one photon processes. For one photon emission, the current in Eq. (29) is such that $s = 0$ and $s = -2$.

Under the conditions of resonance, the one photon stimulated emission amplitude is proportional to

$$J_{-2}\left(\frac{2eV_1}{\hbar\omega_n}\right) \exp(i\Delta\phi) - J_0\left(\frac{2eV_1}{\hbar\omega_n}\right) \exp(-i\Delta\phi) \quad (34)$$

where $0 \leq \Delta\phi \leq 2\pi$.

4.2 The two-photon process

For this process, the Josephson junction-microcavity system is in an initial state such that one photon is present in the cavity and three photons are present in the final state. The initial and final states, therefore, are denoted respectively as

$$\begin{aligned} |I_{st'}\rangle &= |\psi_{J_I}, 1\rangle, \\ |F_{st'}\rangle &= |\psi_{J_F}, 3\rangle. \end{aligned} \quad (35)$$

To second order in perturbation theory, the probability amplitude that the system at time t is in the state $|F_{st'}\rangle$ is²²

$$\langle F_{st'} | \frac{1}{2} \left(-\frac{i}{\hbar} \int_{t_0}^t \hat{H}_i(t') dt' \right)^2 | I_{st'} \rangle \quad (36)$$

Ignoring constants, the amplitude for stimulated emission of the two-photon process is therefore calculated from

$$\int_{t_0}^t dt' \int_{t_0}^{t'} dt'' \int d^3 r' \int d^3 r'' \left[\langle \psi_{J_F} | j(t') j(t'') | \psi_{J_I} \rangle \times \langle 3 | \hat{A}_x^-(z', t') \hat{A}_x^-(z'', t'') | 1 \rangle \right]. \quad (37)$$

The same conditions hold as for the one-photon process. However,

$$\omega_o = 2\omega = 2\omega'. \quad (38)$$

(ω_o is the Josephson frequency, ω is the frequency of the external radiation and ω' is the frequency of the radiation generated by the junction.) For two-photon emission, the current in Eq. (29) is such that $s = -1$ and $s = -3$. The amplitude for stimulated two-photon emission therefore works out to be proportional to

$$\begin{aligned}
& \left(\frac{\omega_n^{1/2} \sin\left(\frac{\omega_n L}{4c_o}\right) \left(1 - \exp\left(-i \frac{\omega_n d}{2c_o}\right)\right)}{\left(1 + r_{21}^* \exp\left(-i \frac{\omega_n d}{c_o}\right)\right)} \right)^2 \exp(-2i\theta') \\
& \times \left[\left(J_{-3}\left(\frac{4eV_1}{\hbar\omega_n}\right) \right)^2 \exp(i2\Delta\phi') + \left(J_{-1}\left(\frac{4eV_1}{\hbar\omega_n}\right) \right)^2 \exp(-i2\Delta\phi') \right. \\
& \quad \left. - 2J_{-3}\left(\frac{4eV_1}{\hbar\omega_n}\right) J_{-1}\left(\frac{4eV_1}{\hbar\omega_n}\right) \right].
\end{aligned} \tag{39}$$

$\Delta\phi'$ is given as

$$\Delta\phi' = \phi_o - 2\theta'. \tag{40}$$

At resonance, the two-photon stimulated emission amplitude is proportional to

$$\left(J_{-3}\left(\frac{4eV_1}{\hbar\omega_n}\right) \right)^2 \exp(i2\Delta\phi') + \left(J_{-1}\left(\frac{4eV_1}{\hbar\omega_n}\right) \right)^2 \exp(-i2\Delta\phi') - 2J_{-3}\left(\frac{4eV_1}{\hbar\omega_n}\right) J_{-1}\left(\frac{4eV_1}{\hbar\omega_n}\right), \tag{41}$$

where $0 \leq \Delta\phi' \leq 2\pi$.

5. Results

We analyse a junction-cavity system for which values of ε , l , L , λ_L and d are taken as 10, 2 nm, 10 μm , 0.05 μm and 150 μm , respectively. From Eqs. (26) and (27), predicted numerical values of the magnetic induction, B_n , and the voltage, V_n , may be calculated for the first five resonant frequencies of the junction-cavity system. These values of B_n and V_n can be used to tune the junction for spontaneous emission of radiation at these specific frequencies.

In the case of stimulated emission, the amplitude in Eq. (34) is used to determine the count rate for the one-photon process and the amplitude in Eq. (41) is used for the two-photon process. In order to find the conditions of resonance, we need to determine the values of the argument of the

Bessel functions ($X' = 2eV_1/\hbar\omega_n$) such that the count rate is a maximum for a given $\Delta\phi$. For the one-photon process, Fig. 3 (a) is a plot of the modulus square of the amplitude against X for $\Delta\phi = 0$. The count rate exhibits a decaying oscillatory dependence on X . The first three values that give a resonance in the count rate are $X = 3.518$, $X = 6.866$ and $X = 10.073$. These values of X are used to find V_1 for a particular resonant frequency of the system. Fig. 3 (b) gives the numerical values of V_1 and ω_n for the three values of X . These predicted values of V_1 and ω_n can be used to tune the junction-cavity system. Fig. 4 (a) is a similar plot to 3 (a) for the two-photon process. This graph displays four values of X' for which the count rate is a maximum – $X'_1 = 1.558$, $X'_2 = 4.888$, $X'_3 = 8.289$ and $X'_4 = 11.530$. While there is also a decaying oscillatory dependence as for the one-photon process, this begins only after the second position of maximum count rate. Fig. 4 (b) gives the numerical values of V_1 that correspond to the first five resonant frequencies of the junction-cavity system. The voltages V_n required to achieve the resonant frequencies for both the one-photon and two-photon processes may be obtained using Eq. (27). Figs. 5 (a) and (b) show the dependence of the stimulated emission count rate on $\Delta\phi$ for the one-photon process and on $\Delta\phi'$ for the two-photon process. There is clearly an oscillatory dependence of the count rate on both parameters $\Delta\phi$ and $\Delta\phi'$.

In Al-Saidi and Stroud's study²³ of a single small underdamped Josephson junction in a large-Q resonant electromagnetic cavity, they employed the full Hamiltonian for the system whereas here, we are interested only in the interaction part of the Hamiltonian. From their analysis they found that for special values of the gate voltage, there was strong interaction between the junction and the resonant photon mode. In this paper it was found that resonance in the emission depended on

the matching of the voltages and magnetic inductions (Eqs. (25) to (27)) for spontaneous emission, and for stimulated emission, on the relation of the voltage induced by the applied field to the potential difference across the junction (which can be determined from the argument of the Bessel function X') and on the relationship between the phase of the applied field and the initial Cooper pair phase difference (Eq. (40)).

6. Conclusion

We have presented a model that describes the emission characteristics of a Josephson junction in a microcavity. For spontaneous emission, we have shown that the magnetic induction, B_n , and voltage, V_n , across the junction must be properly matched to achieve resonance in the cavity. For emission in the microwave region, typical values are of the order of milliteslas for B_n , and millivolts for V_n . For the stimulated emission processes, we calculated the amplitude of the applied radiation, V_1 , necessary to produce maximum count rates for the first five resonant frequencies of the system. We have also shown that to achieve these maximum count rates for the one-photon process, the difference, $\Delta\phi$, between the initial Cooper pair phase difference and the phase of the applied field must be an integral multiple of π , while for the two-photon process, the difference, $\Delta\phi'$, between the initial Cooper pair phase difference and twice the phase of the applied field must be an odd number multiple of $\pi/2$. The ability to control the Josephson junction-cavity system to emit particular numbers of photons, to emit at particular frequencies, and to produce specific count rates as required certainly makes it a versatile source of photons. In particular, single-photon sources will find useful applications in quantum cryptography and information processing.

References

1. H. B. G. Casimir, and D. Polder, “The influence of retardation on the London-van der Waals force,” *Phys. Rev.* **73**, 360-372 (1948).
2. K. H. Drexhage, “Interaction of light with monomolecular dye layers” in *Progress in Optics XII*, E. Wolf, ed. (North Holland, Amsterdam, 1974), p. 163.
3. J. R. Ackerhalt, and J. H. Eberly, “Quantum electrodynamics and radiation reaction: nonrelativistic atomic frequency shifts and lifetimes,” *Phys. Rev. D* **10**, 3350-3375 (1974).
4. D. Meschede, H. Walther, and G. Müller, “The one-atom maser,” *Phys. Rev. Lett.* **54**, 551-554 (1985).
5. R. Arun, and G. S. Agarwal, “Dark states and interferences in cascade transitions of ultracold atoms in a cavity,” *Phys. Rev. A* **66**, 043812-(1-9) (2002).
6. A. Aiello, D. Fargion, and E. Cianci, “Parametric fluorescence and second-harmonic generation in a planar Fabry-Perot microcavity,” *Phys. Rev. A* **58**, 2446-2459 (1998).
7. Y. B. Xie, “Two-level atom and multichromatic waves in a lossless cavity,” *J. Mod. Optics* **44**, 359-378 (1997).
8. A. Carollo, M. F. Santos, and V. Vedral, “Berry’s phase in cavity QED: Proposal for observing an effect of field quantisation,” *Phys. Rev. A* **67**, 063804-(1-4) (2003).
9. D. R. Tilley, “Superradiance in arrays of superconducting weak links,” *Phys. Lett.* **33A**, 205-206 (1970).
10. D. Rogovin, and M. Scully, “Superconductivity and macroscopic quantum phenomena,” *Phys. Rep.* **25C**, 175-291 (1976).
11. P. Barbara, A. B. Cawthorne, S. V. Shitov, and C. J. Lobb, “Stimulated emission and amplification in Josephson junction arrays,” *Phys. Rev. Lett.* **82**, 1963-1966 (1999).

12. Y. B. Xie, "Superconducting Josephson junction of finite capacitance in a lossless cavity: a plausible two-level system with a giant coupling constant," *J. Mod. Optics* **45**, 2025-2038 (1998).
13. W. A. Al-Saidi, and D. Stroud, "Several small Josephson junctions in a resonant cavity: Deviation from the Dicke model," *Phys. Rev. B* **65**, 224512-(1-10) (2002).
14. E. Almaas, and D. Stroud, "Theory of two-dimensional Josephson arrays in a resonant cavity," *Phys. Rev. B* **67**, 064511-(1-12) (2003).
15. D. Rogovin, M. O. Scully, and P. Lee, *Quantum Theory of Josephson Radiation* (Pergamon Press, 1973), p. 241.
16. F. De Martini, M. Marrocco, P. Mataloni, L. Crescentini, and R. Loudon, "Spontaneous emission in the optical microscopic cavity," *Phys. Rev. A* **43**, 2480-2497 (1991).
17. D. Rogovin, "The Josephson junction as a macroscopic radiating atom," *Annals of Phys.* **90**, 18-47 (1975).
18. B. D. Josephson, "Possible new effects in superconductive tunnelling," *Phys. Lett.* **1**, 251-253 (1962).
19. J. C. Swihart, "Field solution for a thin-film superconducting strip transmission line," *J. Appl. Phys.* **32**, 461-469 (1961)
20. R. E. Eck, D. J. Scalapino, and B. N. Taylor, "Self-detection of the ac Josephson current," *Phys. Rev. Lett.* **13**, 15-18 (1964)
21. A. Barone and G. Paterno, *Physics and Applications of the Josephson Effect* (Wiley and Sons, 1982), p. 238.
22. R. J. Glauber, "Optical coherence and photon statistics" in *Quantum optics and electronics*, C. De Witt, A. Blandin, and C. Cohen-Tannoudji, eds. (Gordon and Breach, New York, 1965), p. 79.

23. W. A. Al-Saidi and D. Stroud, "Eigenstates of a small Josephson junction coupled to a resonant cavity," Phys. Rev. B **65**, 014512-(1-7) (2001).

List of Figure Captions

Fig. 1. Schematic of a tunnel or S-I-S (S – superconductor, I – insulator) Josephson junction in a microcavity.

Fig. 2. Geometry of the Fabry-Perot microcavity. 1 and 2 represent the left and right mirrors, respectively, of the microcavity.

Fig. 3. Graphs illustrating the numerical values for the one-photon process of (a) X for the first three positions of maximum count rate for $\Delta\varphi = 0$, and (b) V_1 for the first five cavity resonances of the system for $X_1 = 3.518$, $X_2 = 6.866$ and $X_3 = 10.073$ and $\Delta\varphi = 0$.

Fig. 4. Graphs illustrating the numerical values for the two-photon process of (a) X for the first four positions of maximum count rate for $\Delta\varphi' = 0$, and (b) V_1 for the first five cavity resonances of the system for $X'_1 = 1.558$, $X'_2 = 4.888$, $X'_3 = 8.289$ and $X'_4 = 11.530$ and $\Delta\varphi' = 0$.

Fig. 5 Graph illustrating the variation of the count rate with (a) $\Delta\varphi$, where $\Delta\varphi = \phi_o - \theta'$, for the one-photon process and (b) $\Delta\varphi'$, where $\Delta\varphi' = \phi_o - 2\theta'$, for the two-photon process.

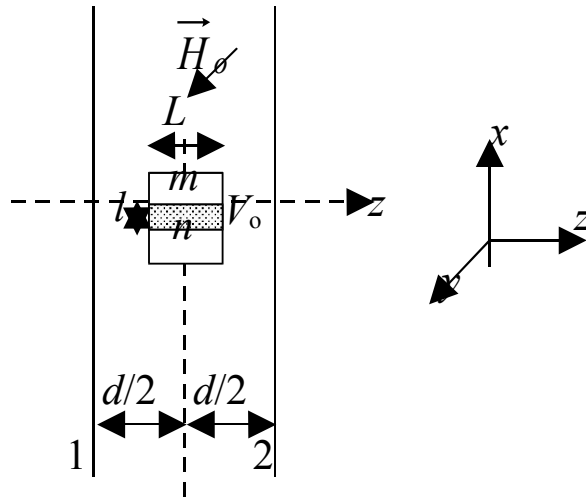


Fig. 1

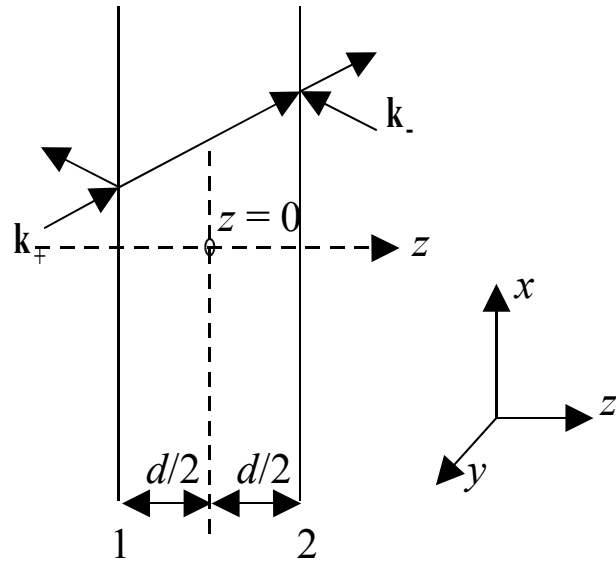


Fig. 2

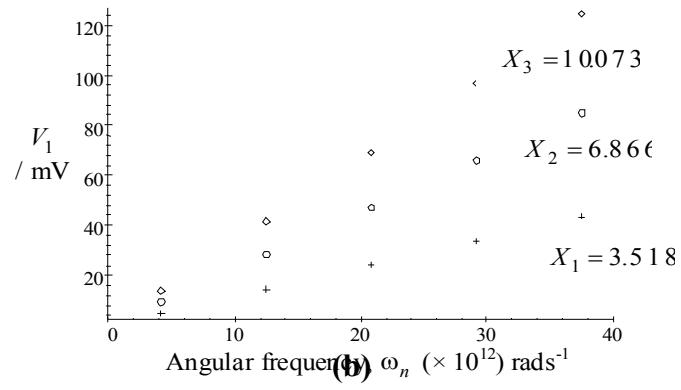
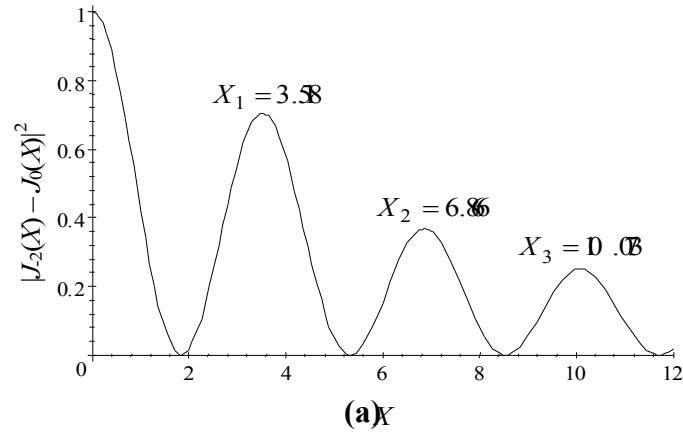


Fig. 3

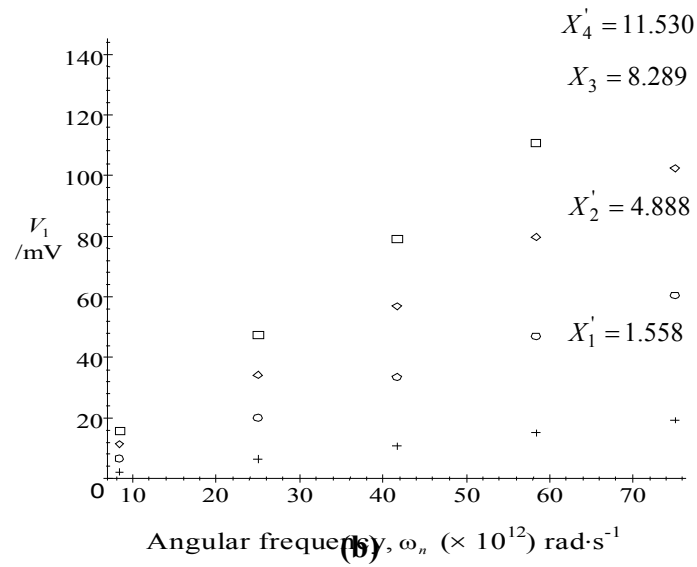
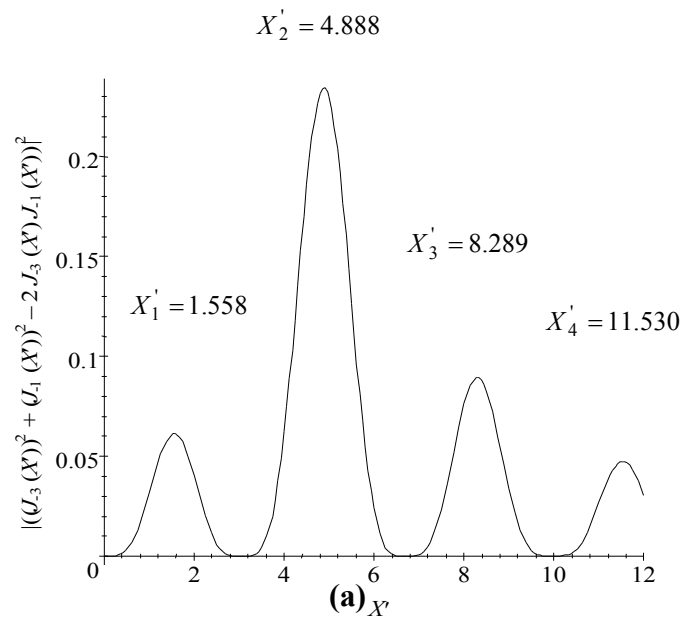


Fig. 4

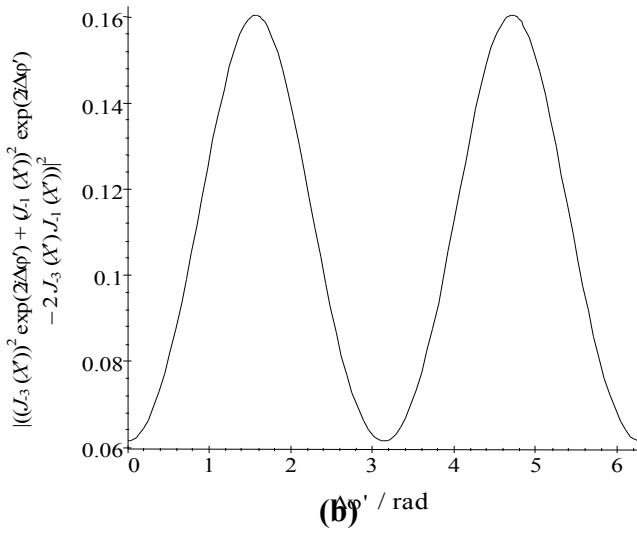
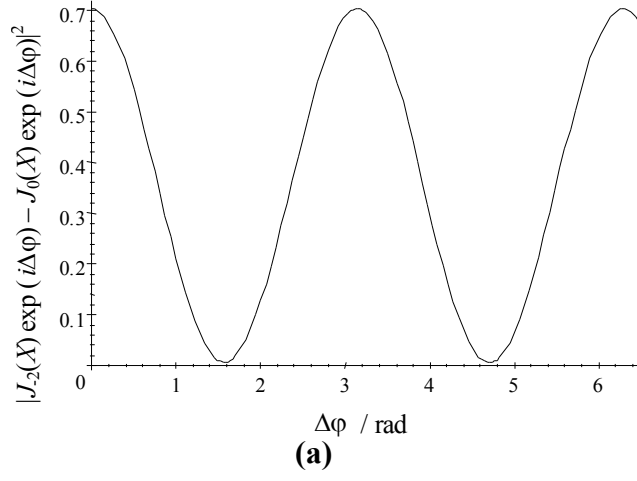


Fig. 5